***Response to Anonymous Referee #1***

*****We thank Referee #1 for their comments and address each below. Our author responses are denoted after each referee comment with **.***

Combining a box model and chamber experiments, the authors of this work provide constraints to the condensed-phase IEPOX reaction kinetics which lack experimental determination. The rate constants of a series of reactions are estimated by finding the best match to the measured tracer concentrations from filters collected in chamber experiments. Based on the rate constants, SOAformation under atmospherically relevant conditions is simulated, and the authors demonstrate that the results show consistency with a recent field measurement. Given that isoprene is by far the most emitted volatile organic compound species in the global scale, and that the reactions and uptake of IEPOX represent the most important steps of isoprene SOA formation, the current work is valuable and relevant to the scope of ACP. Before the paper is published, the following points should be addressed.

Comment 1
A major weakness of the current work lies in the fact that the rate constants are determined based on a countable number of chamber experiments whose conditions are not fully representative of the ambient atmosphere. A clearer link between the chamber and the ambient conditions should be presented. In particular:

1.1) Are the chamber conditions represent certain ambient conditions? If yes, the authors should mention what types of environment the chamber conditions are intended to simulate. If no, the authors should discuss potential problem of extrapolating the chamber experiments to the ambient.

*****The main difference between the chamber and the atmosphere is the low RH and the lack of gas-phase IEPOX reactions. Given that we are investigating this as an isolated SOA production system, the latter are appropriately not considered. Indeed it is rare for ambient RH to be below 5%. The low RH means that the chamber aerosols have a comparatively small amount of liquid water, and the aerosol constituents are therefore more concentrated. Certainly the rates will change with aerosol liquid water, but, as we state in the manuscript, the rate constants themselves are independent of such RH effects. The vast majority of published chamber studies are performed at low RH. We agree with the referee's implication that higher RH experiments would be preferable, but, as discussed in the manuscript, performing these experiments at higher RH resulted in tracer inconsistencies that prevented such studies. Relatedly, at higher RH, the formation of hydrolysis products (i.e., 2-methyltetrols) may be too heavily favored, making it more difficult to obtain detectable quantities of the other tracers on the filters.***

1.2) The authors can probably consider putting the ambient condition used in the simulation in Sect. 3.3 into Table 1 to make a clearer comparison with the conditions employed in the chamber experiments.

*****Table 1 shows initial experimental conditions only. Including initial model conditions for the ambient simulation might cause confusion. Therefore, we chose not to add this information to Table 1.***

1.3) Specifically, the chamber experiments are performed under dry conditions (i.e. RH < 5%), but this seems to be too low to represent the ambient condition. Can rate constants determined from dry

chamber experiment be extrapolate to make implication for the ambient conditions? The authors should justify this in the paper.

***The formation rate constants for the tracers should be independent of RH. Please see the response to Comment 1.1 above regarding the RH of the chamber experiments.***

1.4) In the simulation for ambient condition (Sect. 3.3.), RH is set at 50 %. Is this why 2-methyltetrol is the major SOA constituents in the ambient simulation, but "Other SOA" is the major constituent measured from the chamber? No explanations are provided to discuss the differences.

***The referee is correct that at the higher RH, the hydrolysis product loadings are enhanced. We allude to this Eq. 4 which shows the direct water dependence of the 2-methyltetrols formation rate. We have also added the following statement: "At the increased RH and associated increase in aerosol liquid water, the 2-methyltetrols represent the majority of the formed tracers (see Eq. 4)."***

1.5) The authors mention that the ambient simulation is in "close correspondence to recent [field] measurements" (page 28302, line 3), but they do not seem very close to the reviewer. Why the major SOA constituents in the chamber and the simulation are different (also see the previous comment). Why sulfate titration is significant in the chamber but not under the ambient conditions? The authors should enrich the discussion to explain these differences.

***We did not intend to perfectly simulate the ambient observations. Our intent was to show that for a very general case, we are able to obtain tracer loadings on the same order as observations. We have changed the sentence indicate that the total tracer loading, rather than the distribution of tracers, is in "relatively close correspondence" to recent field studies. We have also added the following qualification: "Keeping in mind that we cannot hope to capture two field studies perfectly for such a general model case,"***
***Sulfate titration is significant in the chamber because of the large amount of IEPOX used compared to the ambient simulation. At the comparatively small IEPOX mixing ratios used in the ambient simulation, there is simply not enough IEPOX to appreciably titrate aerosol sulfate. We have edited the sentence to communicate this: "Additionally, this simulation predicted no appreciable titration of total aqueous inorganic sulfate, suggesting that titration is unlikely to occur in atmospheric sulfate-containing aerosols given expected IEPOX mixing ratios on the order of 1 ppbv."***

Comment 2
Although the approach employed in the current work is robust in constraining rate constants that have not been measured experimentally, discussions about the limitations of this approach seems to be lacking from the current manuscript.

2.1) What are the potential danger of fitting multi-variables to match a countable number of chamber experiments? The authors briefly discuss the experimental limitations of the current work in Sect. 4 (Concluding Remark). Instead of mentioning these in the conclusion, the authors are encouraged to make a new section to summarize the potential shortcomings of the method.

***In requiring all of the rate constants to be positive, all nonphysical solutions to the minimization are not considered, so there is only one solution for each experiment. Any potential shortcomings or limitations stem mainly from method assumptions which are detailed throughout the manuscript in the appropriate sections. Examples include: the lack of authentic standards for tracer quantification in***

***the SOA tracer quantification section, the ability of the AIM model to correctly predict seed aerosol composition in the Model setup and evaluation section, the identity of the "other SOA" in the Model setup and evaluation section and now revisited in the Model-predicted tracer formation kinetics section, the assumption of 100% filter collection/extraction efficiency in the Model setup and evaluation section.***

2.2) The uncertainties associated with the determined rate constants are currently listed as the standard deviation from the five chamber experiments (Table 3), but the uncertainties should be assessed more statistically. When each rate constant is fitted for the best match to the chamber experiment, can a statistical uncertainty be determined for each constant, instead of the standard deviation of the five experiments?

*****As we state in the manuscript, the percent difference between the measured tracers and the model is quite small (<5%), so any statistical uncertainty calculated for the individual experiments would be much smaller than the standard deviation calculated across all of the experiments. Therefore, use of the standard deviations places a more conservative bound on the potential uncertainties than any statistics from the individual experiments.***

2.3) Related to the previous comment, some of the uncertainties (Table 3) are so large that the rate constant can potentially be negative. Explanation should be added to address this issue. In particular, the large uncertainty associated with "Other SOA" formation should be discussed, given that "Other SOA" is the major fraction observed in the chamber experiment (Fig. 3).

*****Indeed the uncertainties in the predicted rate constants for the THFdiols and the "other SOA" are larger than the rate constants. That said, none of the rate constants for any individual experiments were negative, a requirement that we state in the manuscript. This is certainly one of the drawbacks to this approach compared to a more traditional bulk-phase investigation of rate constants such as those described in Eddingsaas et al., (2010) and Cole-Filipiak et al., (2010), where uncertainties are often just the error associated with a curve fit for the kinetic experiment. As we state in our response to Comment 2.2 above, the uncertainties are intended to be as conservative as possible. Please also see our response to Comment 7 from Anonymous Referee #2***

Comment 3
The assumption of "other SOA" being IEPOX-OS should be better justified, or a sensitivity test should be performed. When "Other SOA" is assumed to be a compound with a larger or a smaller molecular weight, would the prediction of the rate constants be altered significantly?

*****To clarify, we do not assume the "other SOA" is IEPOX-OS, only that it is formed from IEPOX-OS. The actual identity of the "other SOA" remains to be determined but, as we state in the manuscript, is likely a combination of both hydroxylated and sulfated products considering results from Lin et al., (2014). As suggested by the referee we have performed additional model runs assuming both a larger (600 g/mole) and smaller (100 g/mole) molecular weight for the "other SOA". These tests are summarized in the added paragraph:***
***"As a sensitivity test to the choice of 334 g mole-1 for the molecular weight of the "other SOA", individual model runs were also performed assuming a molecular weight of 100 and 600 g mole-1. As expected, these tests had the most pronounced effect on the rate constants extracted from simulations with the largest "other SOA" loadings, Exp. No. 1 and 2 (see Table 2). For the 100 g mole-1 case, the resulting adjustment to the rate constants presented in Table 3 was at most a factor of 2.4***

***increase for IEPOX-OS and a 23% decrease, on average, across the remaining rate constants. For the 600 g mole-1 case, all of the rate constants were decreased by 25% on average. Apart from the IEPOX-OS rate constant under the 100 g mole-1 case, which was within 2sigma, all of the rate constants resulting from these sensitivity tests fell within the stated 1sigma uncertainties given in Table 3."***

Comment 4
I found that the information provided in Table 2 repetitive, making this table less informative. The authors are encouraged to find a better way to present the agreement between the actual measurement and modeled results.

*****While we tend to agree with the referee that Table 2 is somewhat repetitive, the main reason we chose to display it as is was to provide readers with tracer loadings from each of the individual experiments. This information could be potentially valuable for other studies investigating IEPOX SOA components. Given the reviewer's comment and considering it is obvious from other figures and the text that the model reproduces the measurements well, we have removed the "model" rows from Table 2.***

Technical comment:
Page 28296 Line 3: "mostly likely" should be "most likely".

*****This change has been made.***

***Response to Anonymous Referee #2***

*****We thank Referee #2 for their comments and address each below. Our author responses are denoted after each referee comment with **.***

The authors show chamber measurements on the formation of secondary organic aerosol (SOA) from isoprene epoxydiols (IEPOX) which they analyze using a kinetic box model in order to determine the elusive bulk reaction rate constants / branching ratios of the acid-catalyzed reactions at work. These reactions are assumed to have high relevance for SOA formation in the troposphere and the topic hence fits nicely within the scope of ACP. I highly appreciate this first attempt to obtain the kinetic rate constants necessary for understanding the chemical system. The paper is well written and the authors discuss their results in the light of previous laboratory experiments and a recent field study. Besides a few minor general comments, I have comments and open questions regarding the modelling part of this study. This paper should be easily publishable in ACP when these last issues are resolved.

Comment 1
The authors decided to use a zero-dimensional model and to prescribe the uptake coefficient γ. Recent modelling studies use 1D models and include adsorption/desorption of trace components explicitly, yielding time-dependent uptake coefficients (e.g. Wilson et al. (2012), Shiraiwa et al. (2013), Roldin et al. (2014)). Also gas diffusion might be a relevant factor at these values of γ. The authors correctly point out in the text that γ may change over time as organics accumulate in the particle phase. Since a more in-depth analysis might be out of the scope of the paper and could be dealt with in a follow-up study, I would suggest mentioning the difficulties that arise when using these models generally used in similar applications that led to their choice of a rather simple box model.

*****Gas diffusion may play a slight limiting role given the γ, and we have neglected any such effects in the results presented here. The effects of gas-phase diffusion would be most pronounced at large γ and particle sizes. Gaston et al. (2014) found only a slight effect (<10%) for this gas-aerosol system, and other systems with similar γ and aerosol sizes have reported minor effects (<3.5%) as well (Thornton et al., 2003). We have added the following statement to address this and reference the 1D models mentioned by the referee: "This approach neglects gas-phase diffusion – the effects of which are expected to be minor for the γ and particles sizes involved here (Gaston et al., 2014; Thornton et al., 2003). Aerosol-phase diffusion, adsorption/desorption of aerosol components, and other potential limitations that, while uncertain, have been explored in 1-D model studies for other systems are also not considered (Roldin et al., 2014; Shiraiwa et al., 2013; Wilson et al., 2012)."***

Comment 2
Do the authors consider changes in the total surface area of the aerosol phase due to particle growth and wall losses? It seems particle growth is strong enough to affect the uptake rates (in the form of kHet in this paper) over time. Would this change the predicted aerosol mass loading as shown in Fig. 1?

*****We state that, "Aerosol surface area was held constant at initial seed aerosol levels over the course of a model run, and thus khet is insensitive to additional surface area resulting from IEPOX-derived SOA." The complete lack of studies regarding the effects of significant aerosol fractions of IEPOX-SOA on γ (or in other words khet) makes determining these effects prohibitively difficult, which we acknowledge unreservedly in the manuscript. Whether or not the particle growth does affect the uptake rate will depend on the nature of the SOA. Water soluble SOA may form homogenously mixed***

***aerosols and enhance or perhaps not appreciably alter khet, whereas a more hydrophobic constituent may limit the uptake through core-shell coating effects such as those discussed by Gaston et al., (2014), which we reference in the manuscript.***

Comment 3
The authors mention two pathways for formation of "other SOA". What are the reasons for only considering the pathway via IEPOX-OS and not via coupling of tetrols?

***As stated in the manuscript, "other SOA" was arbitrarily assumed to come exclusively from IEPOX-OS, even though the formation from tetrols and other reactions is plausible. This was a necessary simplification considering that we are unable to conclusively identify or quantify the individual species that make up the "other SOA".***

Comment 4
Does the H+ concentration ([H+]) change over time in the particle phase due to accumulation of organic material or is it kept constant? I don't see a differential equation taking this into account. Since [H+] factors into every rate constant, it seems like a necessary inclusion.

***[H+] is held constant in the model. Presumably, this is not an oversimplification considering that H+ is a catalyst and should not be consumed by tracer formation. The following statement has been added to the manuscript: "[H+] and [H2O] are held constant over the course of a model run."***
***We are unable to assess whether or not the production IEPOX-SOA could affect [H+] in other ways such as dilution.***

Comment 5
Have the authors considered partitioning of semi-volatile products (such as tetrols) between gas and particle phase? This might skew the final product distribution considerably and not captured by reaction R8. On another note: Is reaction R8 not also acid-catalyzed?

***The measured tracers are assumed to be essentially nonvolatile with any semi-volatile losses captured in Reactions R8 and the absence of these species on the collected filters. Given the lack of gas-phase tracer measurements and the uncertainty of parameters like effective Henry's Law constants for the tracers, such processes have not been considered. As stated in the manuscript, Reaction R8 is treated as a generic first-order loss and carries no pH dependence. We did not presume to know the formation mechanism of these volatile species and as a result, tried to keep the reaction as general as possible.***

Comment 6
The authors mention that reaction rates were "systematically varied" while the model "run in a continuous loop". Could they provide some additional information on how the parameters were obtained? Was it possible to find other sets of kinetic parameter leading to the same modelling result?

***For each loop iteration, the rate constants were adjusted (k's for the first run were an initial guess), the model run, and the sum of the squares of the differences between the model and the measurements was calculated for minimization. MATLAB's Optimization Toolbox functions were used to perform the minimization. The optimization was ended when the sum of the squares of the differences was suitably low – all modeled tracers differed from the measured tracers by <5%. By***

***requiring the rate constants to be positive there were no other values that led to the same model solution. We have included additional details in the manuscript.***

Comment 7
The reaction rate constants were obtained through averaging and errors in the determined reaction rate constants were obtained by taking the standard deviation of results returned from different experiments. I find this procedure of obtaining rate constants highly questionable since an average rate constant from a very limited number of experiments might not be physical at all, especially if the spread between these rate constants is very large (which seems to be the case as indicated by the negative lower bounds of reaction rate coefficients). Why should the kinetic rate constants vary between the experiments at all? Is it possible to find a "global fit" to all experimental data (cf. discussion in Berkemeier et al. (2013)), leading to a unique solution?

*****The referee is correct in stating that kinetic rate constants should not, in theory, vary between the experiments. Averaging model outputs for a single initial experimental condition (seed loading and IEPOX injection amounts) would result in the smaller stated uncertainties, but we chose to represent the formation reactions as conservatively as possible by using different initial experimental conditions while insuring that there was reproducibility for a single initial condition. Requiring the rate constants to be positive ensured that the extracted rate constants were physical. While the standard deviation of the rate constants for the THFdiols and "other SOA" does exceed the mean, in reporting the standard deviation we err on the conservative side for the reported uncertainty. Admittedly, a Monte Carlo type simulation suggested by the referee may serve to reduce the uncertainty in the rate constants. However, the approach presented here is intended to be as unambiguous and straightforward as possible.***

Comment 8
I am confused by the comparison of the obtained rate constants to literature values (p. 28300) and maybe I am misunderstanding this paragraph. If Pye et al. (2013) use a water concentration of 55 M to obtain a third–order rate constant, how does this compare to the third-order rate constant in this paper, which include H+ as third body in the reaction? Is this 3-body reaction rate itself expected to be dependent on pH? How much would it change in the atmospheric case? I would suggest revising this paragraph for better readability.

*****The rate constant obtained by Pye et al. (2013) which is derived from Eddingsaas et al. (2010) is directly comparable to the rate constant that we report. The same reaction, Reaction R1, is being described in both. While the aqueous-phase reaction mechanism to form the 2-methyltetrols is multistep, it is generally represented as an overall 3-body reaction by neglecting the formation of short-lived intermediates – a common practice. We have added text to this paragraph to communicate this is for the overall reaction.***

Comment 9
Could the authors elaborate how much of the deviation of ϕSOA from unity can be attributed to wall losses of (i) IEPOX and (ii) products? How strongly does this affect the wall-free atmospheric case? Can the authors give a clearer picture of all factors governing ϕSOA (in their model / in general)?

*****The IEPOX wall-loss and the aerosol wall-loss will both have similar effects on φSOA: as wall-losses increase, φSOA decreases. In this regard the following statement describing the factors that influence φSOA has also been added: "As described by Matsunaga and Ziemann (2010) and Zhang et al., (2014),***

***wall-losses of VOC and SOA material can effectively decrease calculated φSOA for chamber studies. Considering the IEPOX and aerosol wall-loss rate constants provided above, the corrections for these experiments are minor (<2% change to φSOA). In general, φSOA should mainly be a function of the availability of nucleophiles, provided there is ample time for uptake and tracer formation (Riedel et al., 2015)."***
***The referee raises an excellent point regarding the inclusion of φSOA for the atmospheric model case. We have added the following to the manuscript: "With the lack of wall-losses and the minor contribution of "other SOA", which lowers φSOA as described above, φSOA will be larger (φSOA = 0.125) for this atmospheric case compared to the chamber simulations."***

Minor Comments:
p. 28293, l. 9 – Please mention here why the growth ceases and that the amount of injected IEPOX will decrease over time.

***We have edited the sentence to read as "The majority of the SOA mass growth occurred within the first hour of the injection period, and after 2h, significant SOA growth had ceased after the majority of IEPOX was injected and reacted."***

p. 28301, l. 4 – Please repeat here what is meant with ϕSOA for better readability.

***This change has been made.***

**References:**
***Thornton, J. A., Braban, C. F., and Abbatt, J. P. D.: N2O5 hydrolysis on sub-micron organic aerosols: the effect of relative humidity, particle phase, and particle size, Physical Chemistry Chemical Physics, 5, 4593-4603, doi: 10.1039/b307498f, 2003.***

***Referee Provided References:***
Berkemeier, T., Huisman, A. J., Ammann, M., Shiraiwa, M., Koop, T., and Pöschl, U.: Kinetic regimes and limiting cases of gas uptake and heterogeneous reactions in atmospheric aerosols and clouds: a general classification scheme, Atmos. Chem. Phys., 13, 6663-6686, 10.5194/acp-13-6663-2013, 2013.

Roldin, P., Eriksson, A. C., Nordin, E. Z., Hermansson, E., Mogensen, D., Rusanen, A., Boy, M., Swietlicki, E., Svenningsson, B., Zelenyuk, A., and Pagels, J.: Modelling non-equilibrium secondary organic aerosol formation and evaporation with the aerosol dynamics, gas- and particle-phase chemistry kinetic multilayer model ADCHAM, Atmos. Chem. Phys., 14, 7953-7993, 10.5194/acp-14-7953-2014, 2014.

Shiraiwa, M., Zuend, A., Bertram, A. K., and Seinfeld, J. H.: Gas-particle partitioning of atmospheric aerosols: interplay of physical state, non-ideal mixing and morphology, Phys. Chem. Chem. Phys., 15, 11441-11453, 10.1039/C3CP51595H, 2013.

Wilson, K. R., Smith, J. D., Kessler, S. H., and Kroll, J. H.: The statistical evolution of multiple generations of oxidation products in the photochemical aging of chemically reduced organic aerosol, Phys. Chem. Chem. Phys., 14, 1468-1479, 10.1039/c1cp22716e, 2012.

# Constraining Condensed-Phase Formation Kinetics of Secondary Organic Aerosol Components from Isoprene Epoxydiols

**Theran P. Riedel[1,a], Ying-Hsuan Lin[1], Zhenfa Zhang[1], Kevin Chu[1], Joel A. Thornton[2], William Vizuete[1], Avram Gold[1], and Jason D. Surratt[1]**

[1]Department of Environmental Sciences and Engineering, Gillings School of Global Public Health, The University of North Carolina at Chapel Hill, Chapel Hill, North Carolina, USA

[2]Department of Atmospheric Sciences, University of Washington, Seattle, Washington, USA

[a]Present address: US Environmental Protection Agency, National Exposure Research Laboratory, Research Triangle Park, North Carolina, USA

Correspondence to: J. D. Surratt (surratt@unc.edu)

## Abstract

Isomeric epoxydiols from isoprene photooxidation (IEPOX) have been shown to produce substantial amounts of secondary organic aerosol (SOA) mass and are therefore considered a major isoprene-derived SOA precursor. Heterogeneous reactions of IEPOX on atmospheric aerosols form various aerosol-phase components or "tracers" that contribute to the SOA mass burden. A limited number of the reaction rate constants for these acid-catalyzed aqueous-phase tracer formation reactions have been constrained through bulk laboratory measurements. We have designed a chemical box model with multiple experimental constraints to explicitly simulate gas- and aqueous-phase reactions during chamber experiments of SOA growth from IEPOX uptake onto acidic sulfate aerosol. The model is constrained by measurements of the IEPOX reactive uptake coefficient, IEPOX and aerosol chamber wall-losses, chamber-measured aerosol mass and surface area concentrations, aerosol thermodynamic model calculations, and offline filter-based measurements of SOA tracers. By requiring the model output to match the SOA growth and offline filter measurements collected during the chamber experiments, we derive estimates of the tracer formation reaction rate constants that have not yet been measured or estimated for bulk solutions.


## 1 Introduction

The gas-phase photooxidation of isoprene (2-methyl-1,3-butadiene), the largest biogenic volatile organic compound (VOC) emitted worldwide (Guenther et al., 2012), yields isomeric isoprene epoxydiols (IEPOX) (Paulot et al., 2009). Subsequent acid-catalyzed multiphase chemistry of IEPOX is a significant source of secondary organic aerosol (SOA) mass (Lin et al., 2012; Surratt et al., 2010). In recent field studies, up to 50% of summertime aerosol mass loadings in the southeastern United States have been attributed to SOA resulting from IEPOX heterogeneous reactions (Budisulistiorini et al., 2013; Budisulistiorini et al., 2015; Lin et al., 2013b). Similar IEPOX-derived SOA influences are expected in areas with large isoprene emissions, such as forests primarily composed of broad-leaf vegetation. As a significant SOA precursor, IEPOX has implications regarding potential climate forcing due to the scattering of incoming radiation and also impacts human health due to its large contribution to $PM_{2.5}$ (particulate matter <2.5 μm in diameter) mass (Chung and Seinfeld, 2002; Dockery et al., 1993).

Gas-phase IEPOX can partition to atmospheric aerosol surface area where it can react with aerosol liquid water and aerosol-phase constituents, including sulfate, nitrate, and organics, to form a variety of lower-volatility organic compounds that can remain in the aerosol and contribute to total aerosol mass. Because their presence establishes IEPOX as the precursor, the particle-phase products are referred to as IEPOX-SOA "tracers" (i.e., "molecular markers"). The efficiency of gas-phase IEPOX removal by aerosol surface area is thought to be largely a function of aerosol acidity and concentration of nucleophiles that can react with accommodated IEPOX by acid-catalyzed oxirane ring opening to yield the tracer compounds (Eddingsaas et al., 2010; Gaston et al., 2014; Nguyen et al., 2014; Piletic et al., 2013; Riedel et al., 2015; Surratt et al., 2007b). Products of the reactions have been proposed to include the 2-methyltetrols (2-methylthreitol and 2-methylerythritol) from addition of water, and the corresponding isomeric sulfate esters (IEPOX-OS) from sulfate addition (Reactions (R1) and (R2)) (Claeys et al., 2004; Surratt et al., 2007a).

$$IEPOX_{(aq)} + H^+ + H_2O \rightarrow 2\text{-}methytetrols + H^+ \quad \text{(R1)}$$

$$IEPOX_{(aq)} + H^+ + SO_4^{2-} \rightarrow IEPOX\text{-OS} + H^+ \quad \text{(R2)}$$

Products of nitrate addition, while observed less often, are also thought to be important in certain cases (Darer et al., 2011; Lin et al., 2012). Additional condensed-phase reactions are thought to form IEPOX-derived dimeric species (2-methyltetrol dimers, OS dimers), isomeric $C_5$-alkene triols, cyclodehydration products (3-methyltetrahydrofuran-3,4-diols (3-MeTHF-3,4-diols)), and higher order oligomers which have also been identified in field and chamber studies (Lin et al., 2012; Lin et al., 2014; Lin et al., 2013b; Wang et al., 2005). In the aerosol phase, these oligomers or other high molecular weight aerosol species may be in dynamic equilibrium with low molecular weight tracers (i.e., equilibrium between monomers and oligomers) (Kolesar et al., 2015). The formation of unsaturated IEPOX-derived oligomers has been linked to brown carbon formation and therefore potential radiative forcing (Lin et al., 2014). General acids, such as bisulfate, can also serve as oxirane ring-opening catalysts, though rates for such reactions tend to be significantly slower than rates for acid catalysis under the majority of aerosol conditions (Eddingsaas et al., 2010; Gaston et al., 2014).

To date, only the formation of IEPOX-derived 2-methyltetrols and/or organosulfates have been investigated through direct bulk kinetic measurements (Cole-Filipiak et al., 2010), the extension of bulk kinetic measurements of surrogate epoxides (Eddingsaas et al., 2010), and computational estimates (Piletic et al., 2013). While the tetrol and IEPOX-OS tracers are responsible for a sizeable fraction of

IEPOX-derived SOA (Lin et al., 2013a; Lin et al., 2013b), the remaining tracer formation reactions have yet to be examined, and accurate estimates would benefit SOA modeling efforts (Karambelas et al., 2014; McNeill et al., 2012; Pye et al., 2013). Here we present an approach that combines chamber experiments, offline quantification of SOA tracers from filter samples using authentic standards, and modeling to estimate the formation reaction rate constants of IEPOX-derived SOA tracers whose formation rates are currently unknown. This has been done for a single seed aerosol system, acidified ammonium sulfate at low relative humidity (RH), but the estimated rate coefficients are anticipated to be independent of the seed aerosol used.

## 2 Methods

### 2.1 Chamber experiments

Experiments were conducted under dark conditions in an indoor 10-$m^3$ Teflon smog chamber at the University of North Carolina at Chapel Hill (UNC) (Lin et al., 2014; Riedel et al., 2015). Acidic ammonium sulfate seed aerosol was injected into the dry (RH <5%) chamber using a custom-built atomizer with an atomizing solution of 0.06 M $(NH_4)_2SO_4$ and 0.06 M $H_2SO_4$ until the desired total aerosol mass concentration was achieved. After seed injection, the chamber was left static for at least 30 minutes to ensure that the seed aerosol concentration was stable and uniformly mixed. IEPOX was then injected into the chamber for 2 hours by passing ~4 L $min^{-1}$ of $N_{2(g)}$ through a glass manifold heated at 60 °C containing 50 – 300 μL of a 100 mg $mL^{-1}$ ethyl acetate solution of *trans-β*-IEPOX (Zhang et al., 2012), the predominant IEPOX isomer (Bates et al., 2014). The majority of the SOA mass growth occurred within the first hour of the injection period, and after 2 hours, significant SOA growth had ceased after the majority of IEPOX was injected and reacted.

Chamber aerosol number distributions, which were subsequently converted to total aerosol surface area and volume concentrations, were measured by a scanning electrical mobility system (SEMS v5.0, Brechtel Manufacturing Inc. – BMI) containing a differential mobility analyzer (DMA, BMI) coupled to a mixing condensation particle counter (MCPC Model 1710, BMI). Total volume concentration of seed aerosols was converted to total mass concentration assuming a density of 1.6 g $mL^{-1}$, in accord with aerosol thermodynamic model outputs described in more detail below, and SOA total volume concentration was converted to total mass concentrations assuming a density of 1.25 g $mL^{-1}$ (Kroll et al.,

2006). The chamber RH and temperature were monitored with a commercial RH/temperature probe (OM-62, Omega Engineering Inc.).

## 2.2 SOA tracer quantification

On completion of IEPOX injection, a filter sample was collected for analysis of the chamber-generated SOA. Aerosols were collected onto 46.2 mm Teflon filters (Part No.: SF17471, Tisch Scientific) in a stainless steel filter holder for 2 hours at ~15 L $min^{-1}$ with a carbon strip denuder (Sunset Labs) upstream of the filter holder. Filters were stored in 20 mL scintillation vials at -20 °C prior to extraction and analysis. Denuder efficiency tests were performed by passing ~500 ppbv of IEPOX in $N_{2(g)}$ at low RH (<5%) through the denuder at 2 L $min^{-1}$. ~80% of IEPOX was removed from the sampling stream under these conditions, as measured by an iodide-adduct high-resolution time-of-flight chemical ionization mass spectrometer (HR-TOF-CIMS, Aerodyne Research Inc.) (Lee et al., 2014). The denuder is expected to be less efficient at the higher flow velocities and shorter residence times during filter collection.

As described in previous studies (Lin et al., 2012; Surratt et al., 2010), IEPOX-derived SOA components were extracted from filters with high-purity methanol prior to analysis. Analysis was performed on a gas chromatograph coupled to a mass spectrometer equipped with an electron ionization source (GC/EI-MS, Hewlett-Packard 5890 Series II GC coupled to a Hewlett-Packard 5971A MS) and an ultra-performance liquid chromatograph/high-resolution quadrupole time-of-flight mass spectrometer equipped with electrospray ionization (UPLC/ESI-HR-QTOFMS, Agilent 6500 Series). 2-Methyltetrols, $C_5$-alkene triols, 3-MeTHF-3,4-diols, and the IEPOX-derived dimer were quantified by GC/EI-MS with prior trimethylsilylation. GC/EI-MS calibrations were performed with authentic 2-methyltetrol and 3-MeTHF-3,4-diol standards (Budisulistiorini et al., 2015; Zhang et al., 2012). In the absence of authentic standards, the triols and dimer were assumed to have the same response factor as the 2-methyltetrols (Lin et al., 2012; Lin et al., 2013b). Aliquots of filter extracts were reconstituted in a 50:50 (v/v) methanol:water mixture from which the IEPOX-OS and IEPOX-derived dimer organosulfate (IEPOX-dimerOS) were quantified using UPLC/ESI-HR-QTOFMS operated in the negative ion mode. An authentic IEPOX-OS standard was used for calibration, and IEPOX-dimerOS was assumed to have the same response factor as the IEPOX-OS standard (Budisulistiorini et al., 2015).

## 2.3 Model setup and evaluation

Reaction kinetics of SOA generation were investigated with a zero-dimensional time-dependent chemical box model incorporating explicit aqueous-phase tracer formation. The model is initialized with the amount of *trans*-$\beta$-IEPOX added to the injection manifold and the measured seed aerosol total surface area and mass concentration. Estimates of the aqueous-phase molar concentrations of the inorganic seed aerosol species ($[H^+]$, $[H_2O]$, $[HSO_4^-]$, $[SO_4^{2-}]$) and the total volume of the aqueous phase were obtained from the Extended AIM Aerosol Thermodynamics Model III (AIM, http://www.aim.env.uea.ac.uk/aim/aim.php) (Clegg et al., 1998; Wexler and Clegg, 2002). The composition of the atomizer solution was used as the AIM inputs with a RH of 10%, as AIM does not allow RH inputs <10%. As is typical with aerosol thermodynamic model calculations, the aerosol components were treated as a metastable solution thereby suppressing the formation of solid-phase species (Hennigan et al., 2015). Given the low chamber RH and the composition of the atomizer solution, the seed aerosol was highly acidic, and this assumption is likely valid (Cziczo et al., 1997; Seinfeld and Pandis, 2006). While some gas-phase measurements might be used to constrain aerosol thermodynamic models like AIM, such measurements (e.g., gas-phase ammonia) were unavailable for this study. Furthermore, the actual state of aerosols at low RH is difficult to represent in such models. As a consequence, estimates presented here may be limited by the ability of so-called "reverse mode" thermodynamic aerosol model calculations to appropriately represent the aerosols in the chamber.

A constant IEPOX-aerosol reaction probability ($\gamma$) of 0.021 was assumed over the course of modeled experiments, which is consistent with that measured for similar seed aerosol systems (Gaston et al., 2014; Riedel et al., 2015). The resulting pseudo-first order heterogeneous uptake rate coefficient ($k_{het}$) of IEPOX to the aerosol phase was then calculated by Eq. (1),

$$k_{het} = \frac{\gamma S_a \omega}{4} \quad (1)$$

where $S_a$ is the total seed aerosol surface area concentration and $\omega$ is the mean molecular speed of gas-phase IEPOX. This approach neglects gas-phase diffusion – the effects of which are expected to be minor for the $\gamma$ and particles sizes involved here (Gaston et al., 2014; Thornton et al., 2003). Aerosol-phase diffusion, adsorption/desorption of aerosol components, and other potential limitations that, while uncertain, have been explored in 1-D model studies for other systems are also not considered (Roldin et al., 2014; Shiraiwa et al., 2013; Wilson et al., 2012). Once IEPOX has partitioned to the particle phase

(IEPOX$_{(aq)}$) it is allowed to react with the aerosol constituents to form the SOA tracer species. In addition to Reactions (R1) and (R2), the model incorporates acid-catalyzed reactions to form $C_5$-alkene triols, 3-MeTHF-3,4-diols, IEPOX-dimer, and IEPOX-dimerOS – Reactions (R3) – (R6) below. The model also tracks the formation of "other SOA" – defined as the difference between the chamber-measured SOA mass and the sum of the quantified tracer mass loadings – comprised of unidentified SOA products, most~~ly~~ likely from acid-catalysis, as is the case for the other IEPOX tracers. Species comprising "other SOA" may be oligomers formed by acid-catalyzed coupling of tetrols or IEPOX-OS with IEPOX concomitant with reactive uptake (Lin et al., 2014). Since we are unable to differentiate the extent to which the "other SOA" is formed from these two, or other, pathways, the model assumes all of the "other SOA" is formed from reactions of IEPOX-OS with IEPOX (Reaction (R7)) and has a molecular weight of 334 g mole$^{-1}$, the same as that of IEPOX-dimerOS.

$$IEPOX_{(aq)} + H^+ \rightarrow C_5\text{-alkene triols} + H^+ \quad \text{(R3)}$$

$$IEPOX_{(aq)} + H^+ \rightarrow \text{3-MeTHF-3,4-diols} + H^+ \quad \text{(R4)}$$

$$IEPOX_{(aq)} + H^+ + \text{2-methyltetrols} \rightarrow \text{IEPOX-dimer} + H^+ \quad \text{(R5)}$$

$$IEPOX_{(aq)} + H^+ + IEPOX\text{-OS} \rightarrow \text{IEPOX-dimerOS} + H^+ \quad \text{(R6)}$$

$$IEPOX_{(aq)} + H^+ + IEPOX\text{-OS} \rightarrow \text{other SOA} + H^+ \quad \text{(R7)}$$

The coupled differential equations corresponding to the production and/or loss of IEPOX$_{(g)}$, IEPOX$_{(aq)}$, 2-methyltetrols, IEPOX-OS, $C_5$-alkene triols, 3-MeTHF-3,4-diols, IEPOX-dimer, IEPOX-dimerOS, "other SOA", $HSO_4^-$, and $SO_4^{2-}$ are integrated over the entire IEPOX injection duration (2 hours) or until the observed chamber SOA mass concentration had reached a maximum. [$H^+$] and [$H_2O$] are held constant over the course of a model run. Under the assumption that $HSO_4^-$ is converted to $SO_4^{2-}$ as $SO_4^{2-}$ forms IEPOX-OS, the equilibrium ratio ($R_{SO_4} \equiv SO_4^{2-}/HSO_4^-$) is held constant. Additionally, a general first-order loss, Reaction (R8) from the formation of volatile products that do not contribute to the overall SOA mass, is applied to IEPOX$_{(aq)}$.

$$IEPOX_{(aq)} \rightarrow \text{volatile products} \quad \text{(R8)}$$

This reaction lowers the molar SOA yield ($\phi_{SOA}$) below unity. First-order wall-losses estimated for the chamber from a previous study are also applied to gas-phase IEPOX ($k_{wall} = 9.4 \times 10^{-5}$ s$^{-1}$) and all aerosol-

phase species ($k_{wall\text{-}aerosol} = 1 \times 10^{-5}$ s$^{-1}$) (Riedel et al., 2015). The rate of IEPOX injection into the chamber is simulated in the model by an exponential decay of IEPOX in the injection manifold. The decay constant ($\lambda$) was varied between $1 \times 10^{-3}$ s$^{-1}$ – $2 \times 10^{-3}$ s$^{-1}$ as a fitting parameter to better match the timescale of observed SOA growth. However, over the 2-hour duration of the experiment, the value of the decay constant had a negligible effect on the final model-predicted SOA growth.

The complete set of differential equations used to track each individual species in the model is provided in Eq. 2 – 12.

$$\frac{d[IEPOX_{(g)}]}{dt} = \lambda[IEPOX_{(manifold)}] - k_{het}[IEPOX_{(g)}] - k_{wall}[IEPOX_{(g)}] \quad (2)$$

$$\frac{d[IEPOX_{(aq)}]}{dt} = k_{het}[IEPOX_{(g)}] - k_{R1}[IEPOX_{(aq)}][H_2O][H^+] - k_{R2}[IEPOX_{(aq)}[SO_4^{2-}][H^+] - k_{R3}[IEPOX_{(aq)}][H^+] - k_{R4}[IEPOX_{(aq)}][H^+] - k_{R5}[IEPOX_{(aq)}][H^+][tetrol] - k_{R6}[IEPOX_{(aq)}][H^+][IEPOX\text{-}OS] - k_{R7}[IEPOX_{(aq)}][H^+][IEPOX\text{-}OS] - k_{R8}[IEPOX_{(aq)}] - k_{wall\text{-}aerosol}[IEPOX_{(aq)}] \quad (3)$$

$$\frac{d[tetrol]}{dt} = k_{R1}[IEPOX_{(aq)}][H_2O][H^+] - k_{wall\text{-}aerosol}[tetrol] \quad (4)$$

$$\frac{d[IEPOX\text{-}OS]}{dt} = k_{R2}[IEPOX_{(aq)}][SO_4^{2-}][H^+] - k_{wall\text{-}aerosol}[IEPOX\text{-}OS] \quad (5)$$

$$\frac{d[triol]}{dt} = k_{R3}[IEPOX_{(aq)}][H^+] - k_{wall\text{-}aerosol}[triol] \quad (6)$$

$$\frac{d[diolTHF]}{dt} = k_{R4}[IEPOX_{(aq)}][H^+] - k_{wall\text{-}aerosol}[diolTHF] \quad (7)$$

$$\frac{d[dimer]}{dt} = k_{R5}[IEPOX_{(aq)}][H^+][tetrol] - k_{wall\text{-}aerosol}[dimer] \quad (8)$$

$$\frac{d[dimerOS]}{dt} = k_{R6}[IEPOX_{(aq)}][H^+][IEPOX\text{-}OS] - k_{wall\text{-}aerosol}[dimerOS] \quad (9)$$

$$\frac{d[other]}{dt} = k_{R7}[IEPOX_{(aq)}][H^+][IEPOX\text{-}OS] - k_{wall\text{-}aerosol}[other] \quad (10)$$

$$\frac{d[HSO_4^-]}{dt} = -k_{R2}[IEPOX_{(aq)}][H^+][HSO_4^-]R_{SO_4} - k_{wall\text{-}aerosol}[HSO_4^-] \quad (11)$$

$$\frac{d[SO_4^{2-}]}{dt} = k_{R2}[IEPOX_{(aq)}][H^+][HSO_4^-]R_{SO_4} - k_{R2}[IEPOX_{(aq)}][H^+][SO_4^{2-}] - k_{wall\text{-}aerosol}[SO_4^{2-}] \quad (12)$$

Rate constants ($k$) for Reactions (R1) – (R8) were systemically varied until model output closely matched the offline tracer measurements. Initial values were assigned to $k_{R1}$ – $k_{R8}$, and the model run in a continuous loop, varying each rate constant to minimize the sum of the squares of the differences between the filter measurements and model output, under the constraint that all $k$ >0. Functions available in

MATLAB's Optimization Toolbox were used to perform the minimization. Implicitly, this approach assumes that tracer quantitations are robust, a correct representation of IEPOX-derived SOA speciation and mass loading, and that the filter collection and extraction efficiency are 100%.

## 3 Results and discussion

### 3.1 Model output and comparison to chamber data

Five chamber experiments were performed with the low RH $(NH_4)_2SO_4$ + $H_2SO_4$ seed aerosol system. Table 1 lists initial chamber conditions, including seed aerosol surface area and mass loading and the mass of IEPOX placed in the injection manifold. Figure 1 shows aerosol mass data and the corresponding model simulation for one experiment (Exp. No. 1). The initial seed aerosol mass loading is 113 μg $m^{-3}$, and IEPOX injection is initiated at experiment time (t) = 0. SOA mass growth is most rapid for 30 minutes post injection and slows thereafter, reaching a maximum total aerosol mass concentration of ~275 μg $m^{-3}$ at t ≈ 90 minutes. The timescale of SOA growth for other experiments was similar to that in Figure 1. Figure 2 shows the model-predicted aqueous-phase IEPOX concentration for Exp. No. 1. Despite the large amount of IEPOX injected into the chamber, the maximum predicted aqueous-phase IEPOX concentration reaches only 0.92 moles $L^{-1}$ due to rapid formation of the SOA products. For all simulated experiments, the model reproduced the SOA growth well, both the rate and the maximum mass loading. Nevertheless, caution is necessary in interpreting the significance of this agreement since the model parameters are adjusted to maximize the agreement.

Figure 3 compares the modeled evolution of the SOA tracers in Exp. No. 1 to offline measurements of the corresponding tracers., ~~and results~~ Measured tracer mass loadings for all experiments are ~~summarized~~ provided in Table 2. The tracer concentrations predicted by the model agree well with the filter measurements, differing by <5% for all tracers.

The model also predicts significant titration of total aqueous inorganic sulfate species ($[SO_4^{2-}]$ + $[HSO_4^-]$) over the course of each experiment due to the formation of IEPOX-OS, IEPOX-dimerOS, and "other SOA". Sulfate loadings were predicted to drop 36%, 28%, and 27% for the 30 mg, 15 mg, and 5 mg IEPOX injections, respectively. Figure 4 shows the model-predicted sulfate titration for Exp. No. 1 in which sulfate loading drops from an initial value of ~95 μg $m^{-3}$ to ~60 μg $m^{-3}$ at the conclusion of the model run. These titration levels closely match those reported in Surratt et al. (2007a) for a low-$NO_x$ isoprene oxidation experiment with acidified ammonium sulfate seed aerosol.

### 3.2 Model-predicted tracer formation kinetics

The model-predicted tracer formation rate constants for Reactions (R1) – (R7) are given in Table 3. These are averaged over all experiments and the listed errors correspond to one standard deviation. While the aerosols are not *a priori* ideal solutions, comparison of the rate constants obtained in this study to those estimated from prior studies provides useful insights. Eddingsaas et al. (2010) determined the pseudo second-order formation constants for bulk solutions of cis-2,3-epoxybutane-1,4-diol and used the relationship between 2-methyl-2,3-epoxybutane and 2,3-epoxybutane reaction rate constants to estimate those for 2-methyl-2,3-epoxybutane-1,4-diol (*β*-IEPOX). For 2-methyltetrol formation, Pye et al. (2013) used the *β*-IEPOX value ~~estimated by~~from Eddingsaas et al. (2010) and assumed a water concentration of 55 M ~~in order~~ to derive a third-order rate constant with an explicit water dependence. The resulting rate constants are $9 \times 10^{-4}$ $M^{-2}$ $s^{-1}$ for the overall formation reaction of 2-methyltetrol (Reaction (R1)) and $2 \times 10^{-4}$ $M^{-2}$ $s^{-1}$ for the overall formation reaction of IEPOX-OS (Reaction (R2)). A similar treatment can be applied to the pseudo second-order hydrolysis rate constant (2-methyltetrol formation) for a mixture of *cis*- and *trans*-*β*-IEPOX from Cole-Filipiak et al. (2010) to obtain a rate constant of $6.5 \times 10^{-4}$ $M^{-2}$ $s^{-1}$. Purely computational estimates of $5.3 \times 10^{-2}$ $M^{-2}$ $s^{-1}$ and $5.2 \times 10^{-1}$ $M^{-2}$ $s^{-1}$ for 2-methyltetrol and IEPOX-OS, respectively, are also available for comparison (Piletic et al., 2013). Apart from the computational study, these rate constants are of the same order as those predicted by the model, $3.4 \pm 3.2 \times 10^{-4}$ $M^{-2}$ $s^{-1}$ for 2-methyltetrols and $4.8 \pm 3.4 \times 10^{-4}$ $M^{-2}$ $s^{-1}$ for IEPOX-OS, indicating that the model gives a reasonable representation of the kinetics of the multiphase process in light of the low RH, non-ideal conditions in the highly concentrated chamber aerosols.

Epoxide ring-opening reactions by general acids (i.e., bisulfate) have not been explicitly included in the model. The contribution is expected to be negligible as the branching ratio between the bisulfate and $H^+$-catalyzed reaction channels is likely to heavily favor the $H^+$ channel. For example, in Exp. No. 1, ~98% of the epoxide ring-opening is predicted to proceed through the $H^+$-catalyzed channel compared to that of bisulfate.

Aerosol surface area was held constant at initial seed aerosol levels over the course of a model run, and thus $k_{het}$ is insensitive to additional surface area resulting from IEPOX-derived SOA (Riedel et al., 2015). However, the presence of organics such as polyethylene glycol have been shown to lower $\gamma$ and therefore $k_{het}$ (Gaston et al., 2014), and it is unclear whether the presence of IEPOX-derived SOA

components would have a similar effect. A consequence of the constant surface area is that the model does not account for any possible slowing of the uptake rate resulting from increased aerosol organic content. Measurements of $\gamma$ on mixed and pure IEPOX-SOA would be required to resolve this question.

As a sensitivity test to the choice of 334 g mole$^{-1}$ for the molecular weight of the "other SOA", individual model runs were also performed assuming a molecular weight of 100 and 600 g mole$^{-1}$. As expected, these tests had the most pronounced effect on the rate constants extracted from simulations with the largest "other SOA" loadings, Exp. No. 1 and 2 (see Table 2). For the 100 g mole$^{-1}$ case, the resulting adjustment to the rate constants presented in Table 3 was at most a factor of 2.4 increase for IEPOX-OS and a 23% decrease, on average, across the remaining rate constants. For the 600 g mole$^{-1}$ case, all of the rate constants were decreased by 25% on average. Apart from the IEPOX-OS rate constant under the 100 g mole$^{-1}$ case, which was within 2σ, all of the rate constants resulting from these sensitivity tests fell within the stated 1σ uncertainties given in Table 3.

Given the estimates of the tracer formation rate constants, the calculated $k_{het}$, and the model output, the molar SOA yield ($\phi_{SOA}$) can be estimated as the ratio of the sum of the tracer production rates over the $IEPOX_{(g)}$ heterogeneous loss rate (Riedel et al., 2015). Averaged over the five experiments, $\phi_{SOA}$ = 0.078 ± 0.025 (1σ), with the largest $\phi_{SOA}$ from the 5 mg IEPOX injections and the smallest $\phi_{SOA}$ from the 30 mg injections. The drop in $\phi_{SOA}$ with increased IEPOX injection mass is a function of the increased amount of "other SOA" measured in these experiments. The higher molecular weight assumed for the oligomeric products relative to the molecular weight of the tracers requires less IEPOX to be reacted in order to match the total SOA mass loadings, thus driving down $\phi_{SOA}$. As described by Matsunaga and Ziemann (2010) and Zhang et al. (2014), wall-losses of VOC and SOA material can effectively decrease calculated $\phi_{SOA}$ for chamber studies. Considering the IEPOX and aerosol wall-loss rate constants provided above, the corrections for these experiments are minor (<2% change to $\phi_{SOA}$). In general, $\phi_{SOA}$ should mainly be a function of the availability of nucleophiles, provided there is ample time for uptake and tracer formation (Riedel et al., 2015). $\phi_{SOA}$ = 0.078 is similar to that predicted from an independent modeling approach which estimated the $\phi_{SOA}$ for this aerosol system at 0.1 – 0.12 (Riedel et al., 2015). These results indicate that the molar yield of SOA from IEPOX heterogeneous reactions is likely to be significantly <1 for the majority of atmospheric conditions where aerosols are likely to contain more water and be less acidic than in this study.

### 3.3 Atmospheric implications

Figure 5 shows the model output after 6 hours processing time, using as inputs the rate constants from Table 3 and initial atmospheric conditions which might be representative of a daytime summer urban/rural mixed air mass: 50% RH, ~500 pptv gas-phase IEPOX, and 250 $\mu m^2$ $cm^{-3}$ of ammonium bisulfate aerosol surface area, corresponding to an aerosol mass loading of ~10 $\mu g\ m^{-3}$. The model predicts 0.37 $\mu g\ m^{-3}$ of total SOA with the bulk (77%) being 2-methyltetrols, and minor amounts of IEPOX-OS (14%), $C_5$-alkene triols (7%), and 3-MeTHF-3,4-diols (2%). The remaining tracers – IEPOX-dimer, IEPOX-dimerOS, and "other SOA" – are predicted to form in small amounts (<0.6 ng $m^{-3}$). At the increased RH and associated increase in aerosol liquid water, the 2-methyltetrols represent the majority of the formed tracers (see Eq. 4). With the lack of wall-losses and the minor contribution of "other SOA", which lowers $\phi_{SOA}$ as described above, $\phi_{SOA}$ will be larger ($\phi_{SOA}$ = 0.125) for this atmospheric case compared to the chamber simulations. Additionally, this simulation predicted no appreciable titration of total aqueous inorganic sulfate, suggesting that titration is unlikely to occur in atmospheric sulfate-containing aerosols given expected IEPOX mixing ratios on the order of 1 ppbv.~~, and the rate of sulfated tracer formation is rarely, if ever, limited by the availability of aerosol sulfate.~~

Keeping in mind that we cannot hope to capture two field studies perfectly for such a general model case, ~~T~~the model total IEPOX tracer loading predictions are in relatively close correspondence to recent measurements in the southeastern United States. Analysis of tracers in ambient $PM_{2.5}$ collected by high-volume sampling during summer 2010 in Yorkville, GA, determined that 2-methyltetrols (330 ng $m^{-3}$), $C_5$-alkene triols (290 ng $m^{-3}$), and IEPOX-OS (72 ng $m^{-3}$) were major constituents, with minor amounts of 3-MeTHF-3,4-diols (27 ng $m^{-3}$), IEPOX-dimerOS (5 ng $m^{-3}$), and IEPOX-dimer (0.5 ng $m^{-3}$) (Lin et al., 2012). IEPOX tracer mass loadings from analysis of high-volume $PM_{2.5}$ samples collected at Look Rock, TN, in summer 2013 as part of the Southern Oxidant and Aerosol Study (SOAS) were also dominated by IEPOX-OS (169.5 ng $m^{-3}$), 2-methyltetrols (163.1 ng $m^{-3}$), and $C_5$-alkene triols (144.4 ng $m^{-3}$), whereas 3-MeTHF-3,4-diols (4.4 ng $m^{-3}$) and IEPOX-dimerOS (1.4 ng $m^{-3}$) made only minor contributions (Budisulistiorini et al., 2015).

## 4 Concluding remarks

Attempts to replicate the chamber experiments at higher RH (50%) resulted in large positive deviations (1.2 – 2.3-fold) in total IEPOX tracer mass loadings compared to measured total aerosol mass

loadings by the SEMS-MCPC. This result precluded the extension of these kinetic studies to include humid conditions. A possible explanation for the enhancement of filter mass loadings could be subsequent reactions at the Teflon filter surface; however, appropriate controls are required to confirm such effects. The deviation in mass loadings at higher RH indicate that artifacts may be introduced into field and chamber measurements during filter collection even when sampling through a carbon strip denuder.

Low molecular weight tracers with significant vapor pressures may be detected as a result of decomposition of SOA products. Such a possibility would dictate caution in adopting the kinetic estimates presented here. The sum of these formation rates would likely represent an upper limit to the formation of such SOA species under the assumption that more than one tracer could potentially be formed from the degradation of these products. However, in the absence of evidence to the contrary, there is general agreement that tracers constitute a large fraction of IEPOX-SOA, and additional investigations are required prior to the proposal that certain SOA tracers represent decomposition products.

In summary, this study is a first approach at placing kinetic constraints on the formation of species that have been quantified in laboratory and field measurements but lack directly measured experimental rate constraints. While bulk solution rate constant estimates are desirable, such measurements pose a challenge when authentic standards are unavailable or when surrogates do not adequately represent the true compounds. Additionally, it is unclear that bulk-phase kinetics can approximate aerosol-phase reactions where non-ideal conditions likely play a role. The flexible approach described here may readily be extended to other SOA production systems known to have atmospheric importance.

This study approximates tracer branching ratios for the currently proposed SOA tracers resulting from IEPOX uptake, a necessary step to predict isoprene-derived SOA production in regional models that guide policy decisions. Additional laboratory studies to identify SOA products and elucidate formation mechanisms are important to ensure that both chamber and field measurements accurately reflect atmospheric processes. Modeling developed on the basis of such experimental systems can then be extended to large-scale models.

**Acknowledgements**

This publication was made possible in part by Environmental Protection Agency (EPA) Grant No. R835404. Its contents are solely the responsibility of the grantee and do not necessarily represent the official views of the EPA. Further, the EPA does not endorse the purchase of any commercial products or

services mentioned in the publication. This work is also funded in part by the National Science Foundation under CHE 1404644 and CHE 1404573 and through a grant from the Texas Commission on Environmental Quality (TCEQ), administered by The University of Texas through the Air Quality Research Program. The contents, findings, opinions and conclusions are the work of the authors and do not necessarily represent findings, opinions or conclusions of the TCEQ. The authors also thank Tianqu Cui and Sri Hapsari Budisulistiorini (UNC) and Felipe Lopez-Hilfiker (UW) for helpful discussions.

## Figure and Table Captions

**Figure 1.** Aerosol mass loadings from IEPOX-SOA Exp. No. 1 and corresponding model output. IEPOX injection starts at experiment time t = 0 minutes.

**Figure 2.** Model output of aqueous-phase IEPOX concentrations during Exp. No. 1 simulation.

**Figure 3.** Model output of IEPOX-SOA tracers (left panel) and the associated filter-based tracer measurements (right panel) for Exp. No. 1. The "other SOA" is calculated as the difference between the chamber-measured aerosol mass loadings and the sum of the filter-based tracer loadings.

**Figure 4.** Model output of predicted titration of total inorganic aerosol sulfate ($[SO_4^{2-}] + [HSO_4^-]$) due to sulfated tracer formation during Exp. No. 1 simulation.

**Figure 5.** Model-predicted IEPOX-SOA tracer distribution and loadings for atmospherically relevant initial conditions.

**Table 1.** Summary of conditions for each chamber SOA experiment.

**Table 2.** T~~Comparison of t~~racer mass loadings ~~and model outputs~~ for each chamber SOA experiment.

**Table 3.** Model-predicted formation reaction rate constants for IEPOX-SOA tracers.

## References


Bates, K. H., Crounse, J. D., St. Clair, J. M., Bennett, N. B., Nguyen, T. B., Seinfeld, J. H., Stoltz, B. M., and Wennberg, P. O.: Gas Phase Production and Loss of Isoprene Epoxydiols, The Journal of Physical Chemistry A, 118, 1237-1246, doi: 10.1021/jp4107958, 2014.

Budisulistiorini, S. H., Canagaratna, M. R., Croteau, P. L., Marth, W. J., Baumann, K., Edgerton, E. S., Shaw, S. L., Knipping, E. M., Worsnop, D. R., Jayne, J. T., Gold, A., and Surratt, J. D.: Real-Time Continuous Characterization of Secondary Organic Aerosol Derived from Isoprene Epoxydiols in Downtown Atlanta, Georgia, Using the Aerodyne Aerosol Chemical Speciation Monitor, Environmental Science & Technology, 47, 5686-5694, doi: 10.1021/es400023n, 2013.

Budisulistiorini, S. H., Li, X., Bairai, S. T., Renfro, J., Liu, Y., Liu, Y. J., McKinney, K. A., Martin, S. T., McNeill, V. F., Pye, H. O. T., Nenes, A., Neff, M. E., Stone, E. A., Mueller, S., Knote, C., Shaw, S. L., Zhang, Z., Gold, A., and Surratt, J. D.: Examining the effects of anthropogenic emissions on isoprene-derived secondary organic aerosol formation during the 2013 Southern Oxidant and Aerosol Study (SOAS) at the Look Rock, Tennessee ground site, Atmos. Chem. Phys., 15, 8871-8888, doi: 10.5194/acp-15-8871-2015, 2015.

Chung, S. H., and Seinfeld, J. H.: Global distribution and climate forcing of carbonaceous aerosols, Journal of Geophysical Research: Atmospheres, 107, AAC 14-11-AAC 14-33, doi: 10.1029/2001JD001397, 2002.

Claeys, M., Graham, B., Vas, G., Wang, W., Vermeylen, R., Pashynska, V., Cafmeyer, J., Guyon, P., Andreae, M. O., Artaxo, P., and Maenhaut, W.: Formation of Secondary Organic Aerosols Through Photooxidation of Isoprene, Science, 303, 1173-1176, doi: 10.1126/science.1092805, 2004.

Clegg, S. L., Brimblecombe, P., and Wexler, A. S.: Thermodynamic Model of the System $H^+$–$NH_4^+$–$Na^+$–$SO_4^{2-}$–$NO_3^-$–$Cl^-$–$H_2O$ at 298.15 K, The Journal of Physical Chemistry A, 102, 2155-2171, doi: 10.1021/jp973043j, 1998.

Cole-Filipiak, N. C., O'Connor, A. E., and Elrod, M. J.: Kinetics of the Hydrolysis of Atmospherically Relevant Isoprene-Derived Hydroxy Epoxides, Environmental Science & Technology, 44, 6718-6723, doi: 10.1021/es1019228, 2010.

Cziczo, D. J., Nowak, J. B., Hu, J. H., and Abbatt, J. P. D.: Infrared spectroscopy of model tropospheric aerosols as a function of relative humidity: Observation of deliquescence and crystallization, Journal of Geophysical Research: Atmospheres, 102, 18843-18850, doi: 10.1029/97JD01361, 1997.

Darer, A. I., Cole-Filipiak, N. C., O'Connor, A. E., and Elrod, M. J.: Formation and Stability of Atmospherically Relevant Isoprene-Derived Organosulfates and Organonitrates, Environmental Science & Technology, 45, 1895-1902, doi: 10.1021/es103797z, 2011.

Dockery, D. W., Pope, C. A., Xu, X., Spengler, J. D., Ware, J. H., Fay, M. E., Ferris, B. G., and Speizer, F. E.: An Association between Air Pollution and Mortality in Six U.S. Cities, New England Journal of Medicine, 329, 1753-1759, doi: doi:10.1056/NEJM199312093292401, 1993.

Eddingsaas, N. C., VanderVelde, D. G., and Wennberg, P. O.: Kinetics and Products of the Acid-Catalyzed Ring-Opening of Atmospherically Relevant Butyl Epoxy Alcohols, The Journal of Physical Chemistry A, 114, 8106-8113, doi: 10.1021/jp103907c, 2010.

Gaston, C. J., Riedel, T. P., Zhang, Z., Gold, A., Surratt, J. D., and Thornton, J. A.: Reactive Uptake of an Isoprene-Derived Epoxydiol to Submicron Aerosol Particles, Environmental Science & Technology, 48, 11178-11186, doi: 10.1021/es5034266, 2014.

Guenther, A. B., Jiang, X., Heald, C. L., Sakulyanontvittaya, T., Duhl, T., Emmons, L. K., and Wang, X.: The Model of Emissions of Gases and Aerosols from Nature version 2.1 (MEGAN2.1): an

463 extended and updated framework for modeling biogenic emissions, Geosci. Model Dev., 5, 1471-
464 1492, doi: 10.5194/gmd-5-1471-2012, 2012.
465 Hennigan, C. J., Izumi, J., Sullivan, A. P., Weber, R. J., and Nenes, A.: A critical evaluation of proxy
466 methods used to estimate the acidity of atmospheric particles, Atmos. Chem. Phys., 15, 2775-
467 2790, doi: 10.5194/acp-15-2775-2015, 2015.
468 Karambelas, A., Pye, H. O. T., Budisulistiorini, S. H., Surratt, J. D., and Pinder, R. W.: Contribution of
469 Isoprene Epoxydiol to Urban Organic Aerosol: Evidence from Modeling and Measurements,
470 Environmental Science & Technology Letters, 1, 278-283, doi: 10.1021/ez5001353, 2014.
471 Kolesar, K. R., Li, Z., Wilson, K. R., and Cappa, C. D.: Heating-induced evaporation of nine different
472 secondary organic aerosol types, Environmental Science & Technology, doi:
473 10.1021/acs.est.5b03038, 2015.
474 Kroll, J. H., Ng, N. L., Murphy, S. M., Flagan, R. C., and Seinfeld, J. H.: Secondary Organic Aerosol
475 Formation from Isoprene Photooxidation, Environmental Science & Technology, 40, 1869-1877,
476 doi: 10.1021/es0524301, 2006.
477 Lee, B. H., Lopez-Hilfiker, F. D., Mohr, C., Kurtén, T., Worsnop, D. R., and Thornton, J. A.: An Iodide-
478 Adduct High-Resolution Time-of-Flight Chemical-Ionization Mass Spectrometer: Application to
479 Atmospheric Inorganic and Organic Compounds, Environmental Science & Technology, 48,
480 6309-6317, doi: 10.1021/es500362a, 2014.
481 Lin, Y.-H., Zhang, Z., Docherty, K. S., Zhang, H., Budisulistiorini, S. H., Rubitschun, C. L., Shaw, S. L.,
482 Knipping, E. M., Edgerton, E. S., Kleindienst, T. E., Gold, A., and Surratt, J. D.: Isoprene
483 Epoxydiols as Precursors to Secondary Organic Aerosol Formation: Acid-Catalyzed Reactive
484 Uptake Studies with Authentic Compounds, Environmental Science & Technology, 46, 250-258,
485 doi: 10.1021/es202554c, 2012.
486 Lin, Y.-H., Zhang, H., Pye, H. O. T., Zhang, Z., Marth, W. J., Park, S., Arashiro, M., Cui, T.,
487 Budisulistiorini, S. H., Sexton, K. G., Vizuete, W., Xie, Y., Luecken, D. J., Piletic, I. R., Edney,
488 E. O., Bartolotti, L. J., Gold, A., and Surratt, J. D.: Epoxide as a precursor to secondary organic
489 aerosol formation from isoprene photooxidation in the presence of nitrogen oxides, Proceedings
490 of the National Academy of Sciences, 110, 6718-6723, doi: 10.1073/pnas.1221150110, 2013a.
491 Lin, Y.-H., Budisulistiorini, S. H., Chu, K., Siejack, R. A., Zhang, H., Riva, M., Zhang, Z., Gold, A.,
492 Kautzman, K. E., and Surratt, J. D.: Light-Absorbing Oligomer Formation in Secondary Organic
493 Aerosol from Reactive Uptake of Isoprene Epoxydiols, Environmental Science & Technology,
494 48, 12012-12021, doi: 10.1021/es503142b, 2014.
495 Lin, Y. H., Knipping, E. M., Edgerton, E. S., Shaw, S. L., and Surratt, J. D.: Investigating the influences
496 of SO2 and NH3 levels on isoprene-derived secondary organic aerosol formation using conditional
497 sampling approaches, Atmos. Chem. Phys., 13, 8457-8470, doi: 10.5194/acp-13-8457-2013,
498 2013b.
499 Matsunaga, A., and Ziemann, P. J.: Gas-Wall Partitioning of Organic Compounds in a Teflon Film
500 Chamber and Potential Effects on Reaction Product and Aerosol Yield Measurements, Aerosol
501 Science and Technology, 44, 881-892, doi: 10.1080/02786826.2010.501044, 2010.
502 McNeill, V. F., Woo, J. L., Kim, D. D., Schwier, A. N., Wannell, N. J., Sumner, A. J., and Barakat, J. M.:
503 Aqueous-Phase Secondary Organic Aerosol and Organosulfate Formation in Atmospheric
504 Aerosols: A Modeling Study, Environmental Science & Technology, 46, 8075-8081, doi:
505 10.1021/es3002986, 2012.
506 Nguyen, T. B., Coggon, M. M., Bates, K. H., Zhang, X., Schwantes, R. H., Schilling, K. A., Loza, C. L.,
507 Flagan, R. C., Wennberg, P. O., and Seinfeld, J. H.: Organic aerosol formation from the reactive
508 uptake of isoprene epoxydiols (IEPOX) onto non-acidified inorganic seeds, Atmos. Chem. Phys.,
509 14, 3497-3510, doi: 10.5194/acp-14-3497-2014, 2014.

Paulot, F., Crounse, J. D., Kjaergaard, H. G., Kürten, A., St. Clair, J. M., Seinfeld, J. H., and Wennberg, P. O.: Unexpected Epoxide Formation in the Gas-Phase Photooxidation of Isoprene, Science, 325, 730-733, doi: 10.1126/science.1172910, 2009.

Piletic, I. R., Edney, E. O., and Bartolotti, L. J.: A computational study of acid catalyzed aerosol reactions of atmospherically relevant epoxides, Physical Chemistry Chemical Physics, 15, 18065-18076, doi: 10.1039/C3CP52851K, 2013.

Pye, H. O. T., Pinder, R. W., Piletic, I. R., Xie, Y., Capps, S. L., Lin, Y.-H., Surratt, J. D., Zhang, Z., Gold, A., Luecken, D. J., Hutzell, W. T., Jaoui, M., Offenberg, J. H., Kleindienst, T. E., Lewandowski, M., and Edney, E. O.: Epoxide Pathways Improve Model Predictions of Isoprene Markers and Reveal Key Role of Acidity in Aerosol Formation, Environmental Science & Technology, 47, 11056-11064, doi: 10.1021/es402106h, 2013.

Riedel, T. P., Lin, Y.-H., Budisulistiorini, S. H., Gaston, C. J., Thornton, J. A., Zhang, Z., Vizuete, W., Gold, A., and Surratt, J. D.: Heterogeneous Reactions of Isoprene-Derived Epoxides: Reaction Probabilities and Molar Secondary Organic Aerosol Yield Estimates, Environmental Science & Technology Letters, 2, 38-42, doi: 10.1021/ez500406f, 2015.

Roldin, P., Eriksson, A. C., Nordin, E. Z., Hermansson, E., Mogensen, D., Rusanen, A., Boy, M., Swietlicki, E., Svenningsson, B., Zelenyuk, A., and Pagels, J.: Modelling non-equilibrium secondary organic aerosol formation and evaporation with the aerosol dynamics, gas- and particle-phase chemistry kinetic multilayer model ADCHAM, Atmos. Chem. Phys., 14, 7953-7993, doi: 10.5194/acp-14-7953-2014, 2014.

Seinfeld, J. H., and Pandis, S. N.: Atmospheric Chemistry and Physics: From Air Pollution to Climate Change, 2 ed., Wiley-Interscience, Hoboken, New Jersey, USA, 2006.

Shiraiwa, M., Zuend, A., Bertram, A. K., and Seinfeld, J. H.: Gas-particle partitioning of atmospheric aerosols: interplay of physical state, non-ideal mixing and morphology, Physical Chemistry Chemical Physics, 15, 11441-11453, doi: 10.1039/C3CP51595H, 2013.

Surratt, J. D., Kroll, J. H., Kleindienst, T. E., Edney, E. O., Claeys, M., Sorooshian, A., Ng, N. L., Offenberg, J. H., Lewandowski, M., Jaoui, M., Flagan, R. C., and Seinfeld, J. H.: Evidence for Organosulfates in Secondary Organic Aerosol, Environmental Science & Technology, 41, 517-527, doi: 10.1021/es062081q, 2007a.

Surratt, J. D., Lewandowski, M., Offenberg, J. H., Jaoui, M., Kleindienst, T. E., Edney, E. O., and Seinfeld, J. H.: Effect of Acidity on Secondary Organic Aerosol Formation from Isoprene, Environmental Science & Technology, 41, 5363-5369, doi: 10.1021/es0704176, 2007b.

Surratt, J. D., Chan, A. W. H., Eddingsaas, N. C., Chan, M., Loza, C. L., Kwan, A. J., Hersey, S. P., Flagan, R. C., Wennberg, P. O., and Seinfeld, J. H.: Reactive intermediates revealed in secondary organic aerosol formation from isoprene, Proceedings of the National Academy of Sciences, 107, 6640-6645, doi: 10.1073/pnas.0911114107, 2010.

Thornton, J. A., Braban, C. F., and Abbatt, J. P. D.: $N_2O_5$ hydrolysis on sub-micron organic aerosols: the effect of relative humidity, particle phase, and particle size, Physical Chemistry Chemical Physics, 5, 4593-4603, doi: 10.1039/b307498f, 2003.

Wang, W., Kourtchev, I., Graham, B., Cafmeyer, J., Maenhaut, W., and Claeys, M.: Characterization of oxygenated derivatives of isoprene related to 2-methyltetrols in Amazonian aerosols using trimethylsilylation and gas chromatography/ion trap mass spectrometry, Rapid Communications in Mass Spectrometry, 19, 1343-1351, doi: 10.1002/rcm.1940, 2005.

Wexler, A. S., and Clegg, S. L.: Atmospheric aerosol models for systems including the ions H+, NH4+, Na+, SO42−, NO3−, Cl−, Br−, and H2O, Journal of Geophysical Research: Atmospheres, 107, ACH 14-11-ACH 14-14, doi: 10.1029/2001JD000451, 2002.

Wilson, K. R., Smith, J. D., Kessler, S. H., and Kroll, J. H.: The statistical evolution of multiple generations of oxidation products in the photochemical aging of chemically reduced organic aerosol, Physical Chemistry Chemical Physics, 14, 1468-1479, doi: 10.1039/C1CP22716E, 2012.

Zhang, X., Cappa, C. D., Jathar, S. H., McVay, R. C., Ensberg, J. J., Kleeman, M. J., and Seinfeld, J. H.: Influence of vapor wall loss in laboratory chambers on yields of secondary organic aerosol, Proceedings of the National Academy of Sciences, 111, 5802-5807, doi: 10.1073/pnas.1404727111, 2014.

Zhang, Z., Lin, Y. H., Zhang, H., Surratt, J. D., Ball, L. M., and Gold, A.: Technical Note: Synthesis of isoprene atmospheric oxidation products: isomeric epoxydiols and the rearrangement products cis- and trans-3-methyl-3,4-dihydroxytetrahydrofuran, Atmos. Chem. Phys., 12, 8529-8535, doi: 10.5194/acp-12-8529-2012, 2012.

FIGURES and TABLES

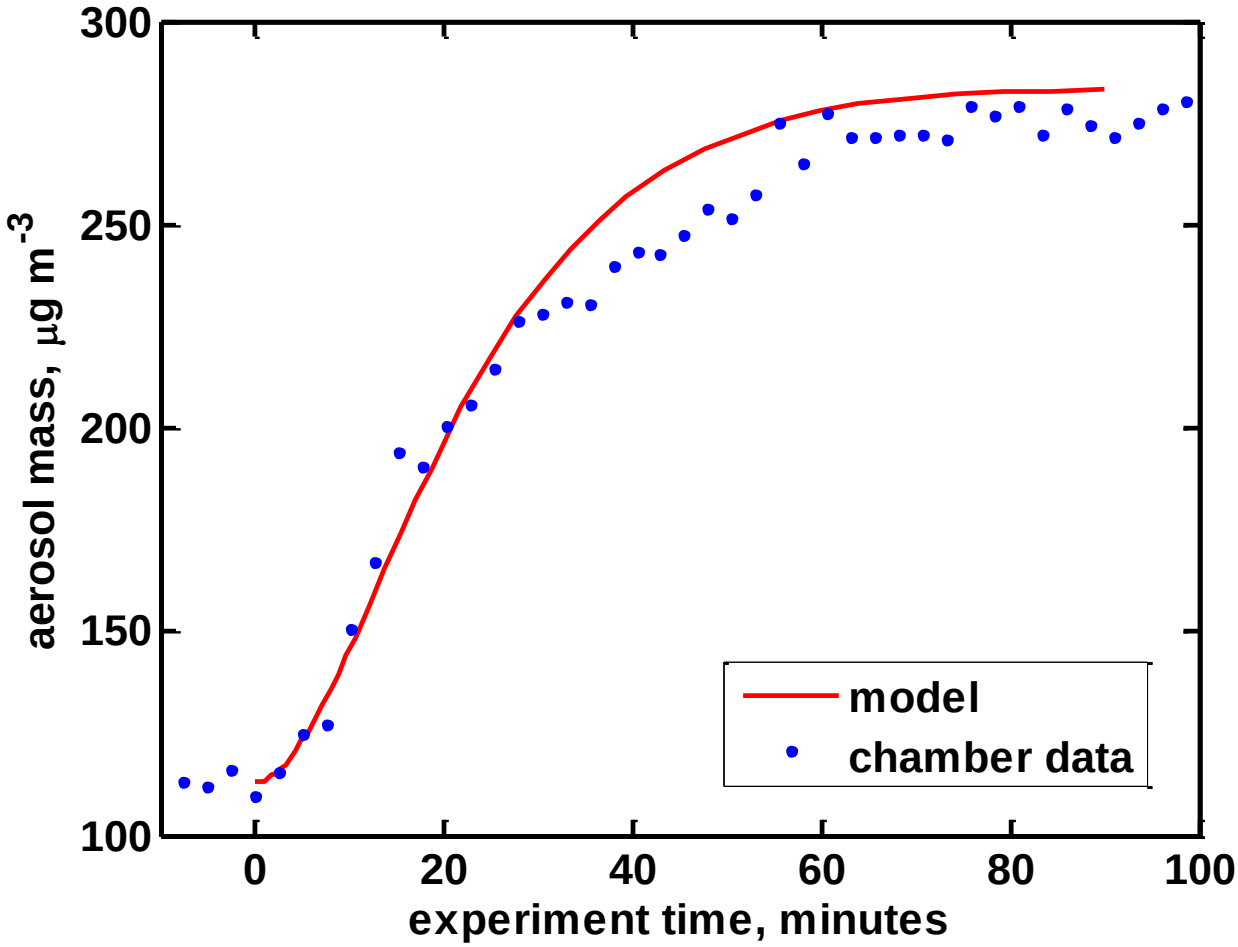


**Figure 1**

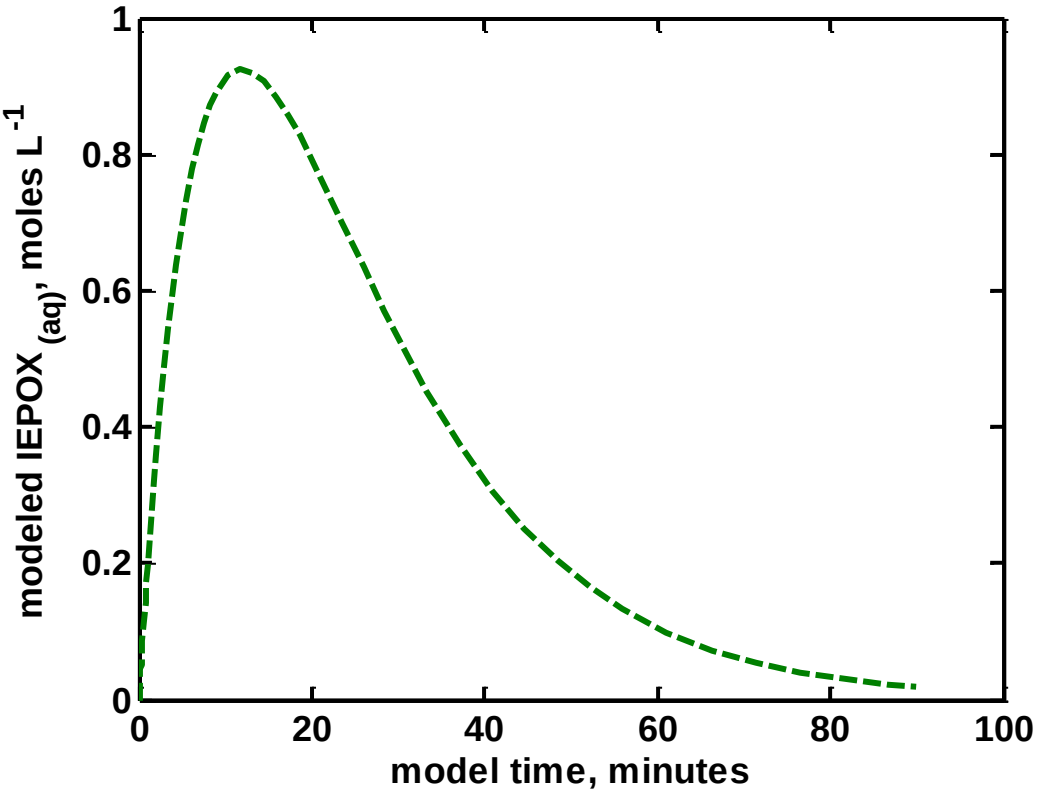


573

574 **Figure 2**

575

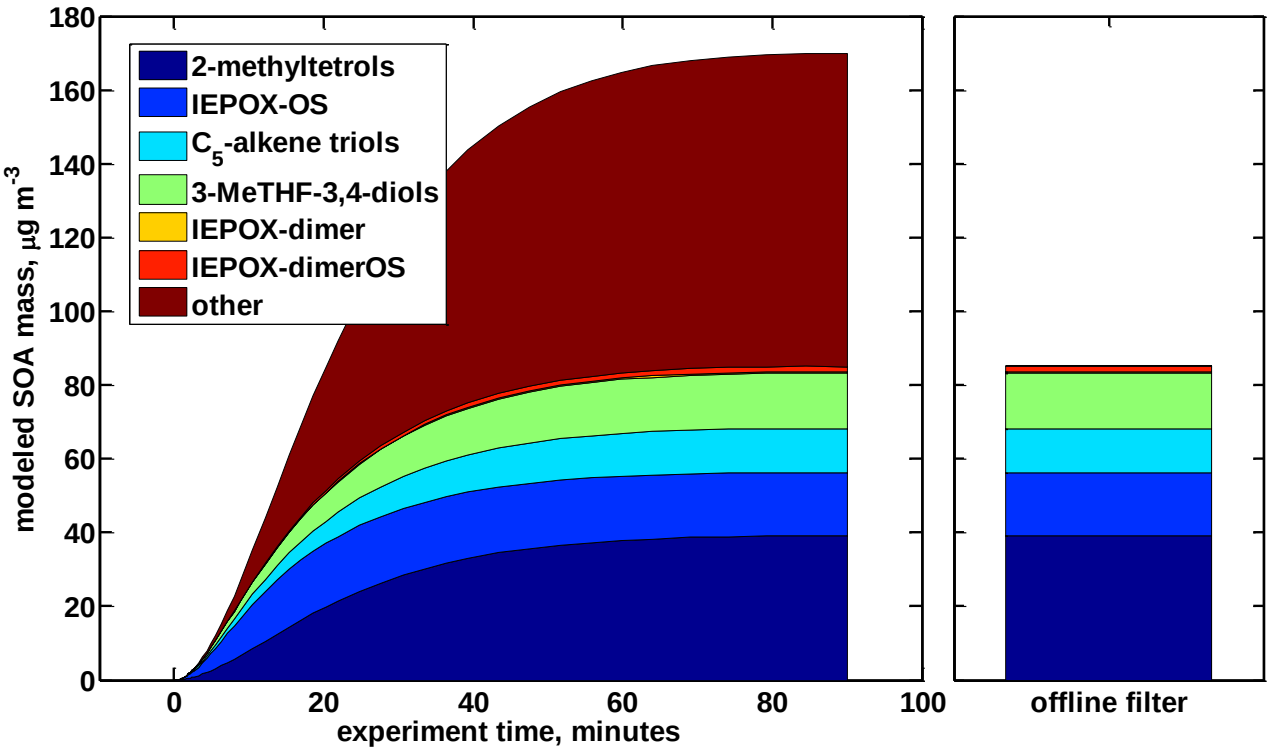


576

577 **Figure 3**

578

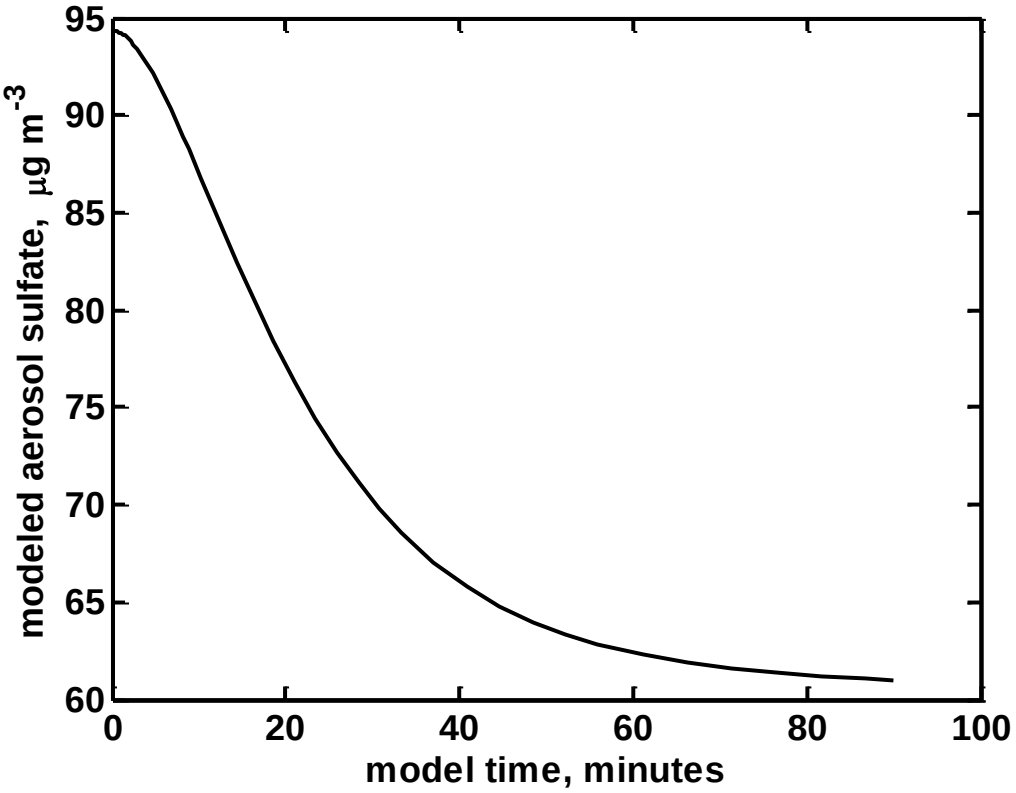


579
580 **Figure 4**

581

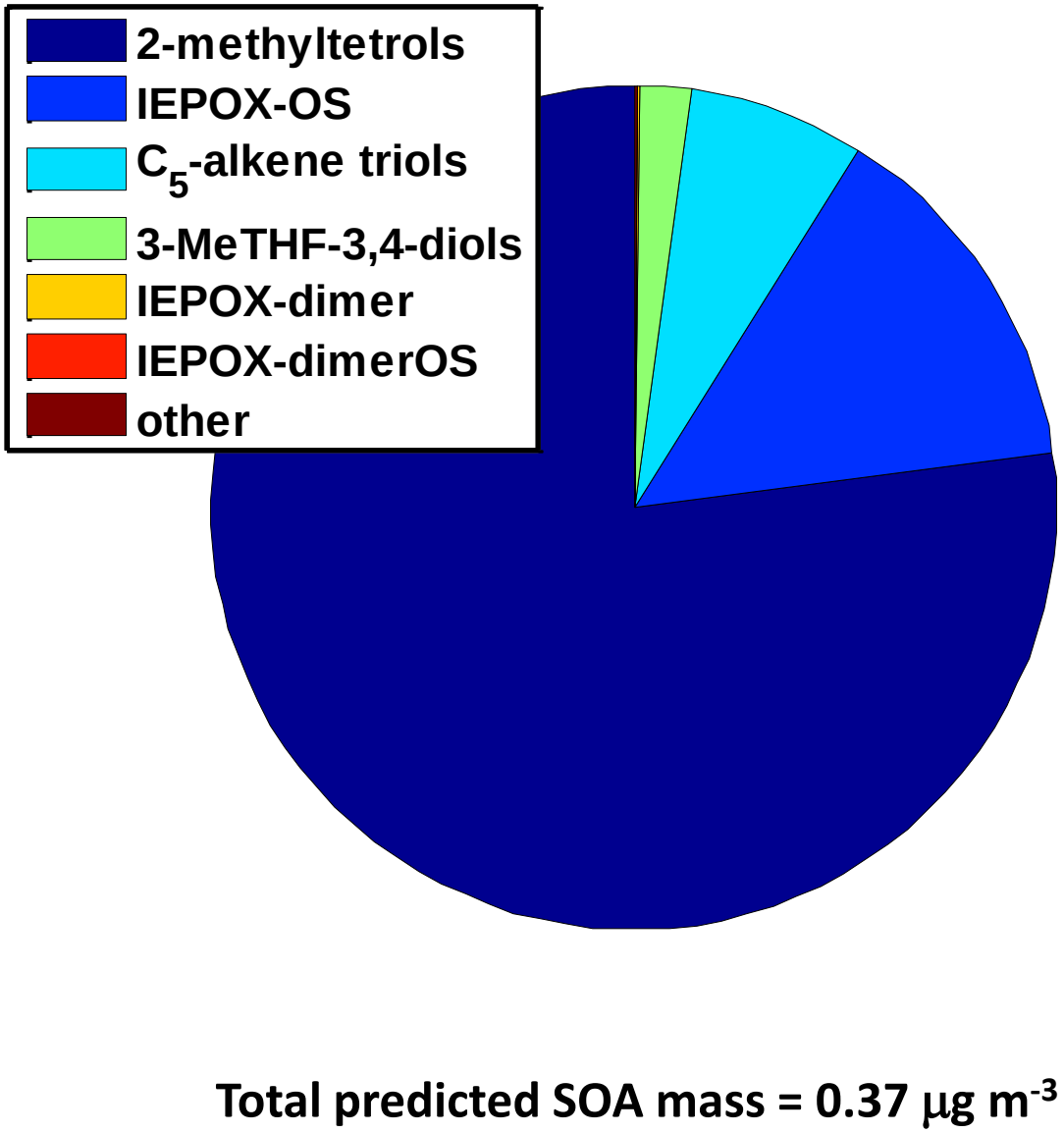


582

583 **Figure 5**

584

| Exp.No. | IEPOX injected/mg | seed surface area/$\mu m^2$ $cm^{-3}$ | seed mass/$\mu g$ $m^{-3}$ |
|---|---|---|---|
| 1 | 30 | 1480 | 113 |
| 2 | 30 | 1660 | 125 |
| 3 | 15 | 1200 | 76 |
| 4 | 5 | 800 | 59 |
| 5 | 5 | 800 | 57 |

585
586 **Table 1**
587

| Exp. No. | Loading/μg $m^{-3}$ | | | | | | | |
|---|---|---|---|---|---|---|---|---|
| | total SOA | 2-methyltetrols | IEPOX-OS | $C_5$-alkene triols | 3-MeTHF-3,4-diols | IEPOX-dimer | IEPOX-dimerOS | other SOA |
| 1 | 170.00 | 39.13 | 16.97 | 12.01 | 15.05 | 0.40 | 1.45 | 84.99 |
| 2 | 185.00 | 41.35 | 23.69 | 12.17 | 13.67 | 0.70 | 3.01 | 90.41 |
| 3 | 131.00 | 34.01 | 13.25 | 35.31 | 3.68 | 3.59 | 4.01 | 37.15 |
| 4 | 60.99 | 3.72 | 27.13 | 18.42 | 0.04 | 0.27 | 10.51 | 0.90 |
| 5 | 63.00 | 3.97 | 27.44 | 19.36 | 0.10 | 0.25 | 9.05 | 2.83 |

588

589 **Table 2**

| SOA tracer formed | k | reaction |
|---|---|---|
| 2-methyltetrols | $3.4\pm3.2 \times 10^{-4}$ $M^{-2}$ $s^{-1}$ | (R1) |
| IEPOX-OS | $4.8\pm3.4 \times 10^{-4}$ $M^{-2}$ $s^{-1}$ | (R2) |
| $C_5$-alkene triols | $8.8\pm3.8 \times 10^{-4}$ $M^{-1}$ $s^{-1}$ | (R3) |
| 3-MeTHF-3,4-diols | $2.6\pm3.5 \times 10^{-4}$ $M^{-1}$ $s^{-1}$ | (R4) |
| IEPOX-dimer | $1.3\pm0.7 \times 10^{-5}$ $M^{-2}$ $s^{-1}$ | (R5) |
| IEPOX-dimerOS | $6.8\pm4.6 \times 10^{-5}$ $M^{-2}$ $s^{-1}$ | (R6) |
| other SOA | $5.7\pm6.9 \times 10^{-4}$ $M^{-2}$ $s^{-1}$ | (R7) |

**Table 3**